

Search for Pair Production of Scalar Top Quarks Decaying to a τ Lepton and a b Quark in $p\bar{p}$ Collisions at $\sqrt{s} = 1.96$ TeV

T. Aaltonen,²³ J. Adelman,¹³ T. Akimoto,⁵⁴ M.G. Albrow,¹⁷ B. Álvarez González,¹¹ S. Amerio,⁴² D. Amidei,³⁴ A. Anastassov,⁵¹ A. Annovi,¹⁹ J. Antos,¹⁴ M. Aoki,²⁴ G. Apollinari,¹⁷ A. Apresyan,⁴⁷ T. Arisawa,⁵⁶ A. Artikov,¹⁵ W. Ashmanskas,¹⁷ A. Attal,³ A. Aurisano,⁵² F. Azfar,⁴¹ P. Azzi-Bacchetta,⁴² P. Azzurri,⁴⁵ N. Bacchetta,⁴² W. Badgett,¹⁷ A. Barbaro-Galtieri,²⁸ V.E. Barnes,⁴⁷ B.A. Barnett,²⁵ S. Baroiant,⁷ V. Bartsch,³⁰ G. Bauer,³² P.-H. Beauchemin,³³ F. Bedeschi,⁴⁵ P. Bednar,¹⁴ S. Behari,²⁵ G. Bellettini,⁴⁵ J. Bellinger,⁵⁸ A. Belloni,²² D. Benjamin,¹⁶ A. Beretvas,¹⁷ J. Beringer,²⁸ T. Berry,²⁹ A. Bhatti,⁴⁹ M. Binkley,¹⁷ D. Bisello,⁴² I. Bizjak,³⁰ R.E. Blair,² C. Blocker,⁶ B. Blumenfeld,²⁵ A. Bocci,¹⁶ A. Bodek,⁴⁸ V. Boisvert,⁴⁸ G. Bolla,⁴⁷ A. Bolshov,³² D. Bortoletto,⁴⁷ J. Boudreau,⁴⁶ A. Boveia,¹⁰ B. Brau,¹⁰ A. Bridgeman,²⁴ L. Brigliadori,⁵ C. Bromberg,³⁵ E. Brubaker,¹³ J. Budagov,¹⁵ H.S. Budd,⁴⁸ S. Budd,²⁴ K. Burkett,¹⁷ G. Busetto,⁴² P. Bussey,²¹ A. Buzatu,³³ K. L. Byrum,² S. Cabrera,¹⁶ M. Campanelli,³⁵ M. Campbell,³⁴ F. Canelli,¹⁷ A. Canepa,⁴⁴ D. Carlsmith,⁵⁸ R. Carosi,⁴⁵ S. Carrillo,¹⁸ S. Carron,³³ B. Casal,¹¹ M. Casarsa,¹⁷ A. Castro,⁵ P. Catastini,⁴⁵ D. Cauz,⁵³ M. Cavalli-Sforza,³ A. Cerri,²⁸ L. Cerrito,³⁰ S.H. Chang,²⁷ Y.C. Chen,¹ M. Chertok,⁷ G. Chiarelli,⁴⁵ G. Chlachidze,¹⁷ F. Chlebana,¹⁷ K. Cho,²⁷ D. Chokheli,¹⁵ J.P. Chou,²² G. Choudalakis,³² S.H. Chuang,⁵¹ K. Chung,¹² W.H. Chung,⁵⁸ Y.S. Chung,⁴⁸ C.I. Ciobanu,²⁴ M.A. Ciocci,⁴⁵ A. Clark,²⁰ D. Clark,⁶ G. Compostella,⁴² M.E. Convery,¹⁷ J. Conway,⁷ B. Cooper,³⁰ K. Copic,³⁴ M. Cordelli,¹⁹ G. Cortiana,⁴² F. Crescioli,⁴⁵ C. Cuenca Almenar,⁷ J. Cuevas,¹¹ R. Culbertson,¹⁷ J.C. Cully,³⁴ D. Dagenhart,¹⁷ M. Datta,¹⁷ T. Davies,²¹ P. de Barbaro,⁴⁸ S. De Cecco,⁵⁰ A. Deisher,²⁸ G. De Lentdecker,⁴⁸ G. De Lorenzo,³ M. Dell'Orso,⁴⁵ L. Demortier,⁴⁹ J. Deng,¹⁶ M. Deninno,⁵ D. De Pedis,⁵⁰ P.F. Derwent,¹⁷ G.P. Di Giovanni,⁴³ C. Dionisi,⁵⁰ B. Di Ruzza,⁵³ J.R. Dittmann,⁴ M. D'Onofrio,³ S. Donati,⁴⁵ P. Dong,⁸ J. Donini,⁴² T. Dorigo,⁴² S. Dube,⁵¹ J. Efron,³⁸ R. Erbacher,⁷ D. Errede,²⁴ S. Errede,²⁴ R. Eusebi,¹⁷ H.C. Fang,²⁸ S. Farrington,²⁹ W.T. Fedorko,¹³ R.G. Feild,⁵⁹ M. Feindt,²⁶ J.P. Fernandez,³¹ C. Ferrazza,⁴⁵ R. Field,¹⁸ G. Flanagan,⁴⁷ R. Forrest,⁷ S. Forrester,⁷ M. Franklin,²² J.C. Freeman,²⁸ I. Furic,¹⁸ M. Gallinaro,⁴⁹ J. Galyardt,¹² F. Garbersen,¹⁰ J.E. Garcia,⁴⁵ A.F. Garfinkel,⁴⁷ K. Genser,¹⁷ H. Gerberich,²⁴ D. Gerdes,³⁴ S. Giagu,⁵⁰ V. Giakoumopolou,⁴⁵ P. Giannetti,⁴⁵ K. Gibson,⁴⁶ J.L. Gimmell,⁴⁸ C.M. Ginsburg,¹⁷ N. Giokaris,¹⁵ M. Giordani,⁵³ P. Giromini,¹⁹ M. Giunta,⁴⁵ V. Glagolev,¹⁵ D. Glenzinski,¹⁷ M. Gold,³⁶ N. Goldschmidt,¹⁸ A. Golossanov,¹⁷ G. Gomez,¹¹ G. Gomez-Ceballos,³² M. Goncharov,⁵² O. González,³¹ I. Gorelov,³⁶ A.T. Goshaw,¹⁶ K. Goulianos,⁴⁹ A. Gresele,⁴² S. Grinstein,²² C. Grosso-Pilcher,¹³ R.C. Group,¹⁷ U. Grundler,²⁴ J. Guimaraes da Costa,²² Z. Gunay-Unalan,³⁵ C. Haber,²⁸ K. Hahn,³² S.R. Hahn,¹⁷ E. Halkiadakis,⁵¹ A. Hamilton,²⁰ B.-Y. Han,⁴⁸ J.Y. Han,⁴⁸ R. Handler,⁵⁸ F. Happacher,¹⁹ K. Hara,⁵⁴ D. Hare,⁵¹ M. Hare,⁵⁵ S. Harper,⁴¹ R.F. Harr,⁵⁷ R.M. Harris,¹⁷ M. Hartz,⁴⁶ K. Hatakeyama,⁴⁹ J. Hauser,⁸ C. Hays,⁴¹ M. Heck,²⁶ A. Heijboer,⁴⁴ B. Heinemann,²⁸ J. Heinrich,⁴⁴ C. Henderson,³² M. Herndon,⁵⁸ J. Heuser,²⁶ S. Hewamanage,⁴ D. Hidas,¹⁶ C.S. Hill,¹⁰ D. Hirschbuehl,²⁶ A. Hocker,¹⁷ S. Hou,¹ M. Houlden,²⁹ S.-C. Hsu,⁹ B.T. Huffman,⁴¹ R.E. Hughes,³⁸ U. Husemann,⁵⁹ J. Huston,³⁵ J. Incandela,¹⁰ G. Introzzi,⁴⁵ M. Iori,⁵⁰ A. Ivanov,⁷ B. Iyutin,³² E. James,¹⁷ B. Jayatilaka,¹⁶ D. Jeans,⁵⁰ E.J. Jeon,²⁷ S. Jindariani,¹⁸ W. Johnson,⁷ M. Jones,⁴⁷ K.K. Joo,²⁷ S.Y. Jun,¹² J.E. Jung,²⁷ T.R. Junk,²⁴ T. Kamon,⁵² D. Kar,¹⁸ P.E. Karchin,⁵⁷ Y. Kato,⁴⁰ R. Kephart,¹⁷ U. Kerzel,²⁶ V. Khotilovich,⁵² B. Kilminster,³⁸ D.H. Kim,²⁷ H.S. Kim,²⁷ J.E. Kim,²⁷ M.J. Kim,¹⁷ S.B. Kim,²⁷ S.H. Kim,⁵⁴ Y.K. Kim,¹³ N. Kimura,⁵⁴ L. Kirsch,⁶ S. Klimenko,¹⁸ M. Klute,³² B. Knuteson,³² B.R. Ko,¹⁶ S.A. Koay,¹⁰ K. Kondo,⁵⁶ D.J. Kong,²⁷ J. Konigsberg,¹⁸ A. Korytov,¹⁸ A.V. Kotwal,¹⁶ J. Kraus,²⁴ M. Kreps,²⁶ J. Kroll,⁴⁴ N. Krumnack,⁴ M. Kruse,¹⁶ V. Krutelyov,¹⁰ T. Kubo,⁵⁴ S. E. Kuhlmann,² T. Kuhr,²⁶ N.P. Kulkarni,⁵⁷ Y. Kusakabe,⁵⁶ S. Kwang,¹³ A.T. Laasanen,⁴⁷ S. Lai,³³ S. Lami,⁴⁵ S. Lammel,¹⁷ M. Lancaster,³⁰ R.L. Lander,⁷ K. Lannon,³⁸ A. Lath,⁵¹ G. Latino,⁴⁵ I. Lazzizzera,⁴² T. LeCompte,² J. Lee,⁴⁸ J. Lee,²⁷ Y.J. Lee,²⁷ S.W. Lee,⁵² R. Lefevre,²⁰ N. Leonardo,³² S. Leone,⁴⁵ S. Levy,¹³ J.D. Lewis,¹⁷ C. Lin,⁵⁹ C.S. Lin,²⁸ J. Linacre,⁴¹ M. Lindgren,¹⁷ E. Lipeles,⁹ T.M. Liss,²⁴ A. Lister,⁷ D.O. Litvintsev,¹⁷ T. Liu,¹⁷ N.S. Lockyer,⁴⁴ A. Loginov,⁵⁹ M. Loreti,⁴² L. Lovas,¹⁴ R.-S. Lu,¹ D. Lucchesi,⁴² J. Lueck,²⁶ C. Luci,⁵⁰ P. Lujan,²⁸ P. Lukens,¹⁷ G. Lungu,¹⁸ L. Lyons,⁴¹ J. Lys,²⁸ R. Lysak,¹⁴ E. Lytken,⁴⁷ P. Mack,²⁶ D. MacQueen,³³ R. Madrak,¹⁷ K. Maeshima,¹⁷ K. Makhoul,³² T. Maki,²³ P. Maksimovic,²⁵ S. Malde,⁴¹ S. Malik,³⁰ G. Manca,²⁹ A. Manousakis,¹⁵ F. Margaroli,⁴⁷ C. Marino,²⁶ C.P. Marino,²⁴ A. Martin,⁵⁹ M. Martin,²⁵ V. Martin,²¹ M. Martínez,³ R. Martínez-Ballarín,³¹ T. Maruyama,⁵⁴ P. Mastrandrea,⁵⁰ T. Masubuchi,⁵⁴ M.E. Mattson,⁵⁷ P. Mazzanti,⁵ K.S. McFarland,⁴⁸ P. McIntyre,⁵² R. McNulty,²⁹ A. Mehta,²⁹ P. Mehtala,²³

S. Menzemer^{k, 11} A. Menzione,⁴⁵ P. Merkel,⁴⁷ C. Mesropian,⁴⁹ A. Messina,³⁵ T. Miao,¹⁷ N. Miladinovic,⁶ J. Miles,³² R. Miller,³⁵ C. Mills,²² M. Milnik,²⁶ A. Mitra,¹ G. Mitselmakher,¹⁸ H. Miyake,⁵⁴ S. Moed,²² N. Moggi,⁵ C.S. Moon,²⁷ R. Moore,¹⁷ M. Morello,⁴⁵ P. Movilla Fernandez,²⁸ J. Mülmenstädt,²⁸ A. Mukherjee,¹⁷ Th. Muller,²⁶ R. Mumford,²⁵ P. Murat,¹⁷ M. Mussini,⁵ J. Nachtman,¹⁷ Y. Nagai,⁵⁴ A. Nagano,⁵⁴ J. Naganoma,⁵⁶ K. Nakamura,⁵⁴ I. Nakano,³⁹ A. Napier,⁵⁵ V. Necula,¹⁶ C. Neu,⁴⁴ M.S. Neubauer,²⁴ J. Nielsen^{f, 28} L. Nodulman,² M. Norman,⁹ O. Norriella,²⁴ E. Nurse,³⁰ S.H. Oh,¹⁶ Y.D. Oh,²⁷ I. Oksuzian,¹⁸ T. Okusawa,⁴⁰ R. Oldeman,²⁹ R. Orava,²³ K. Osterberg,²³ S. Pagan Griso,⁴² C. Pagliarone,⁴⁵ E. Palencia,¹⁷ V. Papadimitriou,¹⁷ A. Papaikonomou,²⁶ A.A. Paramonov,¹³ B. Parks,³⁸ S. Pashapour,³³ J. Patrick,¹⁷ G. Pauletta,⁵³ M. Paulini,¹² C. Paus,³² D.E. Pellett,⁷ A. Penzo,⁵³ T.J. Phillips,¹⁶ G. Piacentino,⁴⁵ J. Piedra,⁴³ L. Pinera,¹⁸ K. Pitts,²⁴ C. Plager,⁸ L. Pondrom,⁵⁸ X. Portell,³ O. Poukhov,¹⁵ N. Pounder,⁴¹ F. Prakoshyn,¹⁵ A. Pronko,¹⁷ J. Proudfoot,² F. Ptohos^{h, 17} G. Punzi,⁴⁵ J. Pursley,⁵⁸ J. Rademacker^{c, 41} A. Rahaman,⁴⁶ V. Ramakrishnan,⁵⁸ N. Ranjan,⁴⁷ I. Redondo,³¹ B. Reisert,¹⁷ V. Rekovic,³⁶ P. Renton,⁴¹ M. Rescigno,⁵⁰ S. Richter,²⁶ F. Rimondi,⁵ L. Ristori,⁴⁵ A. Robson,²¹ T. Rodrigo,¹¹ E. Rogers,²⁴ S. Rolli,⁵⁵ R. Roser,¹⁷ M. Rossi,⁵³ R. Rossin,¹⁰ P. Roy,³³ A. Ruiz,¹¹ J. Russ,¹² V. Rusu,¹⁷ H. Saarikko,²³ A. Safonov,⁵² W.K. Sakumoto,⁴⁸ G. Salamanna,⁵⁰ O. Saltó,³ L. Santi,⁵³ S. Sarkar,⁵⁰ L. Sartori,⁴⁵ K. Sato,¹⁷ A. Savoy-Navarro,⁴³ T. Scheidle,²⁶ P. Schlabach,¹⁷ E.E. Schmidt,¹⁷ M.A. Schmidt,¹³ M.P. Schmidt,⁵⁹ M. Schmitt,³⁷ T. Schwarz,⁷ L. Scodellaro,¹¹ A.L. Scott,¹⁰ A. Scribano,⁴⁵ F. Scuri,⁴⁵ A. Sedov,⁴⁷ S. Seidel,³⁶ Y. Seiya,⁴⁰ A. Semenov,¹⁵ L. Sexton-Kennedy,¹⁷ A. Sfyrly,²⁰ S.Z. Shalhout,⁵⁷ M.D. Shapiro,²⁸ T. Shears,²⁹ P.F. Shepard,⁴⁶ D. Sherman,²² M. Shimojima^{n, 54} M. Shochet,¹³ Y. Shon,⁵⁸ I. Shreyber,²⁰ A. Sidoti,⁴⁵ P. Sinervo,³³ A. Sisakyan,¹⁵ A.J. Slaughter,¹⁷ J. Slaunwhite,³⁸ K. Sliwa,⁵⁵ J.R. Smith,⁷ F.D. Snider,¹⁷ R. Snihur,³³ M. Soderberg,³⁴ A. Soha,⁷ S. Somalwar,⁵¹ V. Sorin,³⁵ J. Spalding,¹⁷ F. Spinella,⁴⁵ T. Spreitzer,³³ P. Squillacioti,⁴⁵ M. Stanitzki,⁵⁹ R. St. Denis,²¹ B. Stelzer,⁸ O. Stelzer-Chilton,⁴¹ D. Stentz,³⁷ J. Strologas,³⁶ D. Stuart,¹⁰ J.S. Suh,²⁷ A. Sukhanov,¹⁸ H. Sun,⁵⁵ I. Suslov,¹⁵ T. Suzuki,⁵⁴ A. Taffard^{e, 24} R. Takashima,³⁹ Y. Takeuchi,⁵⁴ R. Tanaka,³⁹ M. Tecchio,³⁴ P.K. Teng,¹ K. Terashi,⁴⁹ J. Thom^{g, 17} A.S. Thompson,²¹ G.A. Thompson,²⁴ E. Thomson,⁴⁴ P. Tipton,⁵⁹ V. Tiwari,¹² S. Tkaczyk,¹⁷ D. Toback,⁵² S. Tokar,¹⁴ K. Tollefson,³⁵ T. Tomura,⁵⁴ D. Tonelli,¹⁷ S. Torre,¹⁹ D. Torretta,¹⁷ S. Tournear,⁴³ W. Trischuk,³³ Y. Tu,⁴⁴ N. Turini,⁴⁵ F. Ukegawa,⁵⁴ S. Uozumi,⁵⁴ S. Vallecorsa,²⁰ N. van Remortel,²³ A. Varganov,³⁴ E. Vataga,³⁶ F. Vázquez^{l, 18} G. Velez,¹⁷ C. Vellidis^{a, 45} V. Veszpremi,⁴⁷ M. Vidal,³¹ R. Vidal,¹⁷ I. Vila,¹¹ R. Vilar,¹¹ T. Vine,³⁰ M. Vogel,³⁶ I. Volobouev^{q, 28} G. Volpi,⁴⁵ F. Würthwein,⁹ P. Wagner,⁴⁴ R.G. Wagner,² R.L. Wagner,¹⁷ J. Wagner-Kuhr,²⁶ W. Wagner,²⁶ T. Wakisaka,⁴⁰ R. Walhny,⁸ S.M. Wang,¹ A. Warburton,³³ D. Waters,³⁰ M. Weinberger,⁵² W.C. Wester III,¹⁷ B. Whitehouse,⁵⁵ D. Whiteson^{e, 44} A.B. Wicklund,² E. Wicklund,¹⁷ G. Williams,³³ H.H. Williams,⁴⁴ P. Wilson,¹⁷ B.L. Winer,³⁸ P. Wittich^{g, 17} S. Wolbers,¹⁷ C. Wolfe,¹³ T. Wright,³⁴ X. Wu,²⁰ S.M. Wynne,²⁹ A. Yagil,⁹ K. Yamamoto,⁴⁰ J. Yamaoka,⁵¹ T. Yamashita,³⁹ C. Yang,⁵⁹ U.K. Yang^{m, 13} Y.C. Yang,²⁷ W.M. Yao,²⁸ G.P. Yeh,¹⁷ J. Yoh,¹⁷ K. Yorita,¹³ T. Yoshida,⁴⁰ G.B. Yu,⁴⁸ I. Yu,²⁷ S.S. Yu,¹⁷ J.C. Yun,¹⁷ L. Zanello,⁵⁰ A. Zanetti,⁵³ I. Zaw,²² X. Zhang,²⁴ Y. Zheng^{b, 8} and S. Zucchelli⁵

(CDF Collaboration*)

¹*Institute of Physics, Academia Sinica, Taipei, Taiwan 11529, Republic of China*

²*Argonne National Laboratory, Argonne, Illinois 60439*

³*Institut de Física d'Altes Energies, Universitat Autònoma de Barcelona, E-08193, Bellaterra (Barcelona), Spain*

⁴*Baylor University, Waco, Texas 76798*

⁵*Istituto Nazionale di Fisica Nucleare, University of Bologna, I-40127 Bologna, Italy*

⁶*Brandeis University, Waltham, Massachusetts 02254*

⁷*University of California, Davis, Davis, California 95616*

⁸*University of California, Los Angeles, Los Angeles, California 90024*

⁹*University of California, San Diego, La Jolla, California 92093*

¹⁰*University of California, Santa Barbara, Santa Barbara, California 93106*

¹¹*Instituto de Física de Cantabria, CSIC-University of Cantabria, 39005 Santander, Spain*

¹²*Carnegie Mellon University, Pittsburgh, PA 15213*

¹³*Enrico Fermi Institute, University of Chicago, Chicago, Illinois 60637*

¹⁴*Comenius University, 842 48 Bratislava, Slovakia; Institute of Experimental Physics, 040 01 Kosice, Slovakia*

¹⁵*Joint Institute for Nuclear Research, RU-141980 Dubna, Russia*

¹⁶*Duke University, Durham, North Carolina 27708*

¹⁷*Fermi National Accelerator Laboratory, Batavia, Illinois 60510*

¹⁸*University of Florida, Gainesville, Florida 32611*

¹⁹*Laboratori Nazionali di Frascati, Istituto Nazionale di Fisica Nucleare, I-00044 Frascati, Italy*

²⁰*University of Geneva, CH-1211 Geneva 4, Switzerland*

- ²¹*Glasgow University, Glasgow G12 8QQ, United Kingdom*
²²*Harvard University, Cambridge, Massachusetts 02138*
²³*Division of High Energy Physics, Department of Physics, University of Helsinki and Helsinki Institute of Physics, FIN-00014, Helsinki, Finland*
²⁴*University of Illinois, Urbana, Illinois 61801*
²⁵*The Johns Hopkins University, Baltimore, Maryland 21218*
²⁶*Institut für Experimentelle Kernphysik, Universität Karlsruhe, 76128 Karlsruhe, Germany*
²⁷*Center for High Energy Physics: Kyungpook National University, Daegu 702-701, Korea; Seoul National University, Seoul 151-742, Korea; Sungkyunkwan University, Suwon 440-746, Korea; Korea Institute of Science and Technology Information, Daejeon, 305-806, Korea; Chonnam National University, Gwangju, 500-757, Korea*
²⁸*Ernest Orlando Lawrence Berkeley National Laboratory, Berkeley, California 94720*
²⁹*University of Liverpool, Liverpool L69 7ZE, United Kingdom*
³⁰*University College London, London WC1E 6BT, United Kingdom*
³¹*Centro de Investigaciones Energeticas Medioambientales y Tecnologicas, E-28040 Madrid, Spain*
³²*Massachusetts Institute of Technology, Cambridge, Massachusetts 02139*
³³*Institute of Particle Physics: McGill University, Montréal, Canada H3A 2T8; and University of Toronto, Toronto, Canada M5S 1A7*
³⁴*University of Michigan, Ann Arbor, Michigan 48109*
³⁵*Michigan State University, East Lansing, Michigan 48824*
³⁶*University of New Mexico, Albuquerque, New Mexico 87131*
³⁷*Northwestern University, Evanston, Illinois 60208*
³⁸*The Ohio State University, Columbus, Ohio 43210*
³⁹*Okayama University, Okayama 700-8530, Japan*
⁴⁰*Osaka City University, Osaka 588, Japan*
⁴¹*University of Oxford, Oxford OX1 3RH, United Kingdom*
⁴²*University of Padova, Istituto Nazionale di Fisica Nucleare, Sezione di Padova-Trento, I-35131 Padova, Italy*
⁴³*LPNHE, Universite Pierre et Marie Curie/IN2P3-CNRS, UMR7585, Paris, F-75252 France*
⁴⁴*University of Pennsylvania, Philadelphia, Pennsylvania 19104*
⁴⁵*Istituto Nazionale di Fisica Nucleare Pisa, Universities of Pisa, Siena and Scuola Normale Superiore, I-56127 Pisa, Italy*
⁴⁶*University of Pittsburgh, Pittsburgh, Pennsylvania 15260*
⁴⁷*Purdue University, West Lafayette, Indiana 47907*
⁴⁸*University of Rochester, Rochester, New York 14627*
⁴⁹*The Rockefeller University, New York, New York 10021*
⁵⁰*Istituto Nazionale di Fisica Nucleare, Sezione di Roma 1, University of Rome "La Sapienza," I-00185 Roma, Italy*
⁵¹*Rutgers University, Piscataway, New Jersey 08855*
⁵²*Texas A&M University, College Station, Texas 77843*
⁵³*Istituto Nazionale di Fisica Nucleare, University of Trieste/ Udine, Italy*
⁵⁴*University of Tsukuba, Tsukuba, Ibaraki 305, Japan*
⁵⁵*Tufts University, Medford, Massachusetts 02155*
⁵⁶*Waseda University, Tokyo 169, Japan*
⁵⁷*Wayne State University, Detroit, Michigan 48201*
⁵⁸*University of Wisconsin, Madison, Wisconsin 53706*
⁵⁹*Yale University, New Haven, Connecticut 06520*

We search for pair production of supersymmetric top quarks (\tilde{t}_1), followed by R -parity violating decay $\tilde{t}_1 \rightarrow \tau b$ with a branching ratio β , using 322 pb^{-1} of $p\bar{p}$ collisions at $\sqrt{s} = 1.96 \text{ TeV}$ collected by the CDF II detector at Fermilab. Two candidate events pass our final selection criteria, consistent with the standard model expectation. We set upper limits on the cross section $\sigma(\tilde{t}_1\bar{\tilde{t}}_1) \times \beta^2$ as a function of the stop mass $m(\tilde{t}_1)$. Assuming $\beta = 1$, we set a 95% confidence level limit $m(\tilde{t}_1) > 153 \text{ GeV}/c^2$. The limits are also applicable to the case of a third generation scalar leptoquark (LQ_3) decaying $LQ_3 \rightarrow \tau b$.

PACS numbers: 12.60.Jv, 14.80.Ly, 13.85.Rm, 11.30.Pb, 11.30.Er

*With visitors from ^aUniversity of Athens, 15784 Athens, Greece,

^bChinese Academy of Sciences, Beijing 100864, China, ^cUniversity

In supersymmetric (SUSY) models [1], the spin-1/2 quarks and leptons have spin-0 quark and lepton partners. Experimental data suggest that the superpartners of the first and second generation are heavier than those of the standard model (SM) particles, while the mass of the lighter scalar top quark (stop or \tilde{t}_1) is weakly constrained and can be below that of the top quark [2]. This is due to the mixing between the left and right handed interaction eigenstates which is a function of the large Yukawa coupling of the top quark. At the Fermilab Tevatron stop quarks and antiquarks can be produced in pairs in strong interactions ($gg/q\bar{q} \rightarrow \tilde{t}_1\bar{\tilde{t}}_1$). A single stop could also be produced at the Tevatron, e.g., via $b\bar{g} \rightarrow \tilde{t}_1\tau$ [3]; however, unlike pair production, this process requires an R -parity (R_p) violating vertex. In regions of parameter space not excluded by data, R_p violating (\mathcal{R}_p) couplings are small [4], making single stop production negligible compared to pair production. Stop quarks can decay into lighter SUSY and SM particles if R_p is conserved or into ordinary quarks and/or leptons if R_p is violated. Within the framework of \mathcal{R}_p SUSY [4], theoretical studies indicate that the dominant decay mode for the light stop is the lepton number violating decay $\tilde{t}_1 \rightarrow \tau b$ for a wide range of SUSY model parameters, including the region allowed by neutrino oscillation data [5].

Leptoquarks appear in various SM extensions [6]. Charge $|Q| = 2/3$ and $|Q| = 4/3$ third generation scalar leptoquarks (LQ_3) are expected to decay into τ and b with $\mathcal{B}(LQ_3 \rightarrow \tau b) = 1$ for all LQ_3 states when $m(LQ_3) < m(t)$. The next-to-leading order (NLO) cross section for $LQ_3\bar{LQ}_3$ production is very close to the $\tilde{t}_1\bar{\tilde{t}}_1$ production cross section $\sigma(\tilde{t}_1\bar{\tilde{t}}_1)$ since diagrams with virtual gluino exchange are strongly suppressed with the existing limits on gluino mass [7]. Thus, the limits obtained for \mathcal{R}_p stop should be fully applicable to the LQ_3 case.

In this Letter we describe a search for $\tilde{t}_1\bar{\tilde{t}}_1 \rightarrow \tau^+\tau^-b\bar{b}$ with the upgraded CDF detector (CDF II) [8] and set an upper limit on $\sigma(\tilde{t}_1\bar{\tilde{t}}_1) \times \beta^2$, neglecting additional decay modes that may pass selections of this analysis when

$\beta \equiv \mathcal{B}(\tilde{t}_1 \rightarrow \tau b) < 1$. We look for a final state with either an electron or muon from the decay $\tau \rightarrow \ell\nu_\ell\nu_\tau$ ($\ell = e$ or μ), a hadronically decaying tau τ_h , missing transverse energy \cancel{E}_T [9] from the neutrinos, and two or more jets. We have studied the addition of a requirement that the jets are consistent with originating from the hadronization of a b quark but found that the increase in purity is outweighed by the loss in signal acceptance. Therefore, we make no such specific requirement. This analysis uses approximately three times more data at a higher \sqrt{s} than the previous CDF result [10] that set a 95% C.L. limit of $m(\tilde{t}_1) > 122 \text{ GeV}/c^2$. The increased \sqrt{s} is expected to give a substantial increase in the $\tilde{t}_1\bar{\tilde{t}}_1$ production rate, e.g., $\sim 35\%$ for $m(\tilde{t}_1) = 155 \text{ GeV}/c^2$.

CDF II features several main subsystems critical to this analysis. The charged particle tracking system consists of multi-layer silicon detectors and an open-cell cylindrical drift chamber enclosed in a 1.4 T superconducting magnet. At $|\eta| < 1$ [9] charged particle trajectories traverse all chamber layers, while at larger $|\eta|$ the chamber coverage is reduced progressively. The calorimeter system is organized into electromagnetic and hadronic sections segmented in a projective tower geometry and covers $|\eta| < 3.6$. A set of strip and wire chambers is located within the central electromagnetic calorimeter at approximately the depth of shower maximum and aids in reconstructing electrons, and photons for $|\eta| < 1.1$. The muon detection system is located outside of the calorimeter and covers $|\eta| < 1.0$.

The analysis begins with a data sample collected by inclusive lepton-plus-track triggers [11]. These triggers select events containing an electron (muon) candidate with $E_T > 8 \text{ GeV}$ ($p_T > 8 \text{ GeV}/c$) and a second track, which is required to be consistent with originating from a tau decay by demanding that there be no other nearby tracks with $p_T > 1.5 \text{ GeV}/c$ between the cones of 0.175 and 0.524 radians around the track. The integrated luminosity of the data sample is $322 \pm 19 \text{ pb}^{-1}$ [12].

From the trigger sample we select events offline by identifying at least one lepton with $p_T^\ell > 10 \text{ GeV}/c$ and at least one τ_h candidate in $|\eta| < 1$. The details of the τ_h identification algorithm can be found in Refs. [13, 14]. We require $p_T^\tau > 15 \text{ GeV}/c$. Jets are reconstructed using a fixed-cone algorithm with $\Delta R \equiv \sqrt{\Delta\eta^2 + \Delta\phi^2} = 0.4$ within $|\eta| < 2.4$.

The dominant SM backgrounds are vector boson production, QCD, and $t\bar{t}$ production. In QCD multijet events, for example, semileptonic b quark decays or γ conversions can be misidentified as lepton candidates, and narrow jets can be misidentified as τ_h candidates. We require the sum of the p_T of the tracks within $\Delta R < 0.4$ around the lepton candidate (I_{trk}) be less than $2 \text{ GeV}/c$, and no jet with $E_T > 15 \text{ GeV}$ within $0.3 < \Delta R < 0.8$ around the lepton. Further, we reject events where the muon or electron candidate is consistent with a cosmic

of Bristol, Bristol BS8 1TL, United Kingdom, ^dUniversity Libre de Bruxelles, B-1050 Brussels, Belgium, ^eUniversity of California Irvine, Irvine, CA 92697, ^fUniversity of California Santa Cruz, Santa Cruz, CA 95064, ^gCornell University, Ithaca, NY 14853, ^hUniversity of Cyprus, Nicosia CY-1678, Cyprus, ⁱUniversity College Dublin, Dublin 4, Ireland, ^jUniversity of Edinburgh, Edinburgh EH9 3JZ, United Kingdom, ^kUniversity of Heidelberg, D-69120 Heidelberg, Germany, ^lUniversidad Iberoamericana, Mexico D.F., Mexico, ^mUniversity of Manchester, Manchester M13 9PL, England, ⁿNagasaki Institute of Applied Science, Nagasaki, Japan, ^oUniversity de Oviedo, E-33007 Oviedo, Spain, ^pQueen Mary, University of London, London, E1 4NS, England, ^qTexas Tech University, Lubbock, TX 79409, ^rIFIC(CSIC-Universitat de Valencia), 46071 Valencia, Spain,

ray muon or γ conversion electron (see Ref. [13] for details). We veto events where the invariant mass of the primary electron (muon) and a reconstructed electron (muon) candidate, which is required to pass loose identification criteria [13], is $76 < m_{\ell\ell} < 106 \text{ GeV}/c^2$. We also reject events with $76 < m_{e\tau} < 106 \text{ GeV}/c^2$ and azimuthal separation of $|\Delta\phi_{e\tau}| > 2.9 \text{ rad}$. For the muon channel we do not apply a similar requirement, as the probability for a muon to be reconstructed as a τ_h is negligible. To suppress further QCD and $Z \rightarrow \tau\tau$ events [10], we require $S_T \equiv |\vec{p}_T^\ell| + |\vec{p}_T^{\tau_h}| + |\vec{E}_T|/c > 110 \text{ GeV}/c$.

We define six regions in the $m_T(\ell, \cancel{E}_T) \equiv \sqrt{2p_T^\ell \cancel{E}_T(1 - \cos\Delta\phi_{\ell, \cancel{E}_T})}$ versus N_{jet} plane, and denote them as A_j (B_j) for $m_T \leq 35 \text{ GeV}/c^2$ ($m_T > 35 \text{ GeV}/c^2$) and $j = 0, 1$ or 2 for $N_{\text{jet}} = 0, 1$ or ≥ 2 . We count into N_{jet} the jet candidates that have $E_T > 20 \text{ GeV}$ and are separated from any of e, μ or τ_h by $\Delta R > 0.8$. The minimal values of S_T and jet E_T are optimized for maximum significance in the A_2 region for $140 - 160 \text{ GeV}/c^2$ \tilde{t}_1 's. The $m_T \leq 35 \text{ GeV}/c^2$ cut effectively separates signal from $W + \text{jet}$ and $t\bar{t}$ backgrounds. The $N_{\text{jet}} \geq 2$ requirement strongly suppresses the Drell-Yan contribution. The data in region A_2 were not examined until the analysis procedure was finalized. The regions with $N_{\text{jet}} = 0$ or 1 contain mostly background and were used mainly as control samples for validation. Region B_2 has an appreciable signal acceptance ($\sim 40\%$ of that in region A_2) but substantially higher background expectation. For statistical interpretation of the data, we developed a likelihood method that, in addition to our primary signal region A_2 , utilizes side-band regions A_0, B_0 , and B_2 , which are used to perform data-driven $W + \text{jet}$ background estimations and to improve the sensitivity of the analysis.

The total event acceptance is $\alpha \equiv \epsilon_{\text{MC}} \cdot \epsilon_{\text{trig}}$. Here ϵ_{MC} is the product of geometrical and kinematical acceptances, efficiencies to identify lepton and τ_h candidates, including isolation requirements, and the efficiency for the all remaining cuts. We use PYTHIA Monte Carlo (MC) generator [15] and the GEANT3-based [16] CDF II detector simulation to calculate ϵ_{MC} . Our nominal choice for the parton distribution functions (PDFs) is CTEQ5L [17] with the renormalization scale $Q \equiv \sqrt{m(\tilde{t}_1)^2 + p_T(\tilde{t}_1)^2}$. The trigger efficiency ϵ_{trig} is measured using data [14]. In region A_2 α increases nearly linearly from about 0.6% at $m(\tilde{t}_1) = 100 \text{ GeV}/c^2$ to 2.7% at $170 \text{ GeV}/c^2$ and is similar for both electron and muon channels.

The combined systematic uncertainty on α decreases almost linearly from 11% for $m(\tilde{t}_1) = 100 \text{ GeV}/c^2$ to 7.2% for $170 \text{ GeV}/c^2$ and is similar in both channels. The largest contribution comes from the PDF systematic uncertainty, which is estimated using the uncertainty sets of CTEQ6.1M PDFs [17] and the technique described in Ref. [18]. For a $150 \text{ GeV}/c^2$ stop this uncertainty on α is

4.0% . The uncertainty due to an imperfect knowledge of the jet energy scale, determined by varying the scale by $\pm 1\sigma$, is 2.9% . The uncertainty due to the amount of initial and final state radiation is found to be 2.5% . Other sources of systematic uncertainty include the uncertainties in lepton and τ_h identification and isolation, and \cancel{E}_T resolution, and amount to a 5.1% relative contribution. The uncertainty on the integrated luminosity is 6% .

The SM backgrounds come from two sources: (i) events with a true $\ell\tau_h$ pair from $Z/\gamma^*(\rightarrow \tau\tau) + \text{jets}$, $t\bar{t}$ and diboson (WW, WZ, ZZ) production; and (ii) events where lepton or τ_h candidates do not originate from a true lepton or tau but from the jets in $W + \text{jet}$, $Z/\gamma^*(\rightarrow \ell\ell) + \text{jets}$ and QCD multijet events. We first estimate the background from SM processes excluding the $W + \text{jet}$ contribution. Drell-Yan, $t\bar{t}$, and WW production are estimated using PYTHIA and the CDF II detector simulation. For Drell-Yan backgrounds we use scale factors that improve the agreement between the prediction for the yield of these events in MC simulation and the yield observed in data. The QCD multijet contribution is estimated by extrapolating the number of observed events in data for events with non-isolated leptons, defined by $2 < I_{\text{trk}} < 10 \text{ GeV}/c$, into the class of events with an isolated lepton, defined by $I_{\text{trk}} < 2 \text{ GeV}/c$ [13]. The NLO cross sections of $6.7 \pm 0.7 \text{ pb}$ [19] and $13.5 \pm 0.5 \text{ pb}$ [20] for $t\bar{t}$ and WW production, respectively, are used. The contributions from WZ and ZZ are found to be negligible.

The PYTHIA MC simulation does not accurately predict the absolute rate of the $W + \text{jet}$ background contribution (N^W) in this analysis. Therefore, to estimate N^W in each region, we use the differences between the data and all other backgrounds plus signal in regions A_2, B_2, A_0 , and B_0 and the assumption that $\mathcal{R} \equiv [N^W(A_2)/N^W(B_2)] \cdot [N^W(B_0)/N^W(A_0)] \sim 1$. The ratios in \mathcal{R} are determined by kinematics of the $W + \text{jet}$ events at fixed N_{jet} and are well modeled in MC. Based on MC predictions and cross checks with data vs MC comparisons, we conclude that $\mathcal{R} = 1.0 \pm 0.5$ is a conservative assumption. We define a likelihood function using Poisson statistics as a function of $\sigma(\tilde{t}_1\tilde{t}_1)$ and N^W . The input parameters to the likelihood are the numbers of observed and expected events in each of the four regions. The number of expected events in region i is given by $N_i = \sigma(\tilde{t}_1\tilde{t}_1) \cdot \mathcal{B}(\tau\tau \rightarrow \ell\tau_h) \cdot \int \mathcal{L} dt \cdot \alpha_i + N_i^{\text{BG}} + N_i^W$, where the branching ratio $\mathcal{B}(\tau\tau \rightarrow \ell\tau_h) \simeq 0.23$, N_i^{BG} includes all SM backgrounds except $W + \text{jet}$ events, and α_i is the total event acceptance for signal in region i . The ratio $\mathcal{R} = 1.0 \pm 0.5$ and N^W in regions A_0, B_0 , and B_2 are nuisance parameters with flat prior distributions. The large uncertainty on \mathcal{R} does not affect our final results because $N^W(A_2)$ is expected to be small. We use this two-dimensional likelihood to estimate N^W for each region and to calculate upper limits on $\sigma(\tilde{t}_1\tilde{t}_1) \times \beta^2$.

In Table I we show the number of events observed

TABLE I: Number of events observed in data, N_{obs} , along with the expected number of SM background events. The $W + \text{jet}$ contributions are shown separately as they are estimated using the observed number of events in the data, the SM prediction excluding the $W + \text{jet}$ contribution, and a possible stop quark contribution.

Reg	$e + \tau_h$ Channel				$\mu + \tau_h$ Channel		
	N_{obs}	SM Backgrounds			N_{obs}	SM Backgrounds	
		Other	$W + \text{jet}$			Other	$W + \text{jet}$
A ₂	1	$2.0^{+0.5}_{-0.4}$	$0^{+0.4}_{-0}$	1	$1.0^{+0.4}_{-0.2}$	$0^{+0.5}_{-0}$	
B ₂	4	$2.8^{+0.5}_{-0.3}$	$1.0^{+2.0}_{-1.0}$	4	$2.3^{+0.4}_{-0.3}$	$1.7^{+2.0}_{-1.5}$	
A ₁	4	$3.3^{+0.5}_{-0.5}$	$0.2^{+1.2}_{-0.2}$	3	$2.6^{+0.6}_{-0.4}$	$0.1^{+0.8}_{-0.1}$	
B ₁	9	$2.3^{+0.4}_{-0.3}$	$6.7^{+3.2}_{-2.7}$	6	$2.3^{+0.5}_{-0.3}$	$3.8^{+2.7}_{-2.1}$	
A ₀	11	$9.1^{+1.2}_{-1.1}$	$1.6^{+2.7}_{-1.6}$	8	$5.2^{+0.7}_{-0.5}$	$2.5^{+2.4}_{-2.1}$	
B ₀	25	$4.5^{+0.7}_{-0.6}$	$21.1^{+5.6}_{-4.3}$	28	$5.4^{+0.8}_{-0.6}$	$23.6^{+4.9}_{-5.7}$	

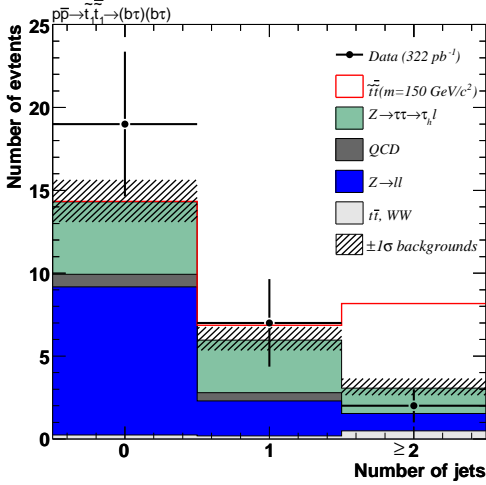


FIG. 1: Distribution of the number of jets ($E_T > 20$ GeV) for events with $m_T(\ell, \ell_T) \leq 35$ GeV/ c^2 (regions A₀, A₁, and A₂) compared to the expectations from SM processes and prediction for $\tilde{t}_1\bar{\tilde{t}}_1$ ($m(\tilde{t}_1) = 150$ GeV/ c^2) signal.

in the data along with the SM expectation. In Fig. 1 we present the N_{jet} distribution for events with $m_T \leq 35$ GeV/ c^2 (regions A₀, A₁, and A₂).

Two events are found in region A₂, consistent with the SM prediction. We use the likelihood function to obtain a probability of such an observation given a specific signal cross section, and calculate a 95% C.L. limit on $\sigma(\tilde{t}_1\bar{\tilde{t}}_1) \times \beta^2$. The electron and muon channels are treated as two separate measurements, taking into account the correlations among the systematic uncertainties.

Figure 2 shows the 95% C.L. limit curves for $\sigma(\tilde{t}_1\bar{\tilde{t}}_1) \times \beta^2$ as a function of $m(\tilde{t}_1)$, with the numerical results given in Table II. The dotted curve is our experimental result, compared to the NLO cross section (solid line) obtained using PROSPINO version 2 [22] with our nominal choice

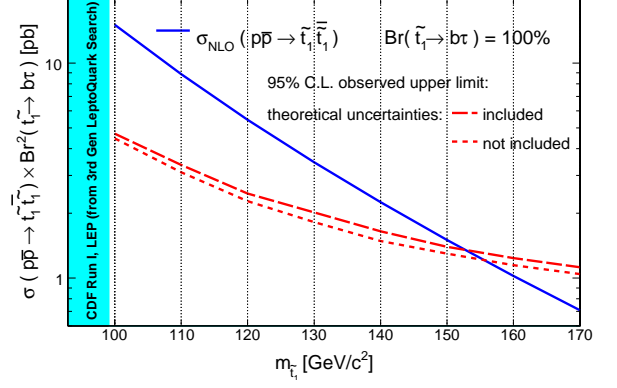


FIG. 2: 95% C.L. limit curves for the $\tilde{t}_1\bar{\tilde{t}}_1$ production cross section times the branching ratio $\tilde{t}_1 \rightarrow b\tau$ squared for the cases when the theoretical uncertainty on the cross section is (dashed line) and is not (dotted line) considered in the limit calculation (see text for details). The previous constraint $m(LQ_3) > 99$ GeV/ c^2 [21] is also shown.

TABLE II: 95% C.L. upper limit on $\sigma(\tilde{t}_1\bar{\tilde{t}}_1) \times \beta^2$ (in pb) as a function of $m(\tilde{t}_1)$ for the cases when uncertainty on the theoretical cross section is considered ($\sigma_{\text{with uncert}}^{95\%} \times \beta^2$) and is not considered ($\sigma_{\text{no uncert}}^{95\%} \times \beta^2$), where $\beta \equiv \mathcal{B}(\tilde{t}_1 \rightarrow \tau b)$.

$m(\tilde{t}_1)$ (GeV/ c^2)	100	110	120	130	140	150	160	170
$\sigma_{\text{with uncert}}^{95\%} \times \beta^2$ (pb)	4.73	3.37	2.50	1.99	1.61	1.38	1.26	1.14
$\sigma_{\text{no uncert}}^{95\%} \times \beta^2$ (pb)	4.48	3.11	2.27	1.81	1.47	1.26	1.16	1.04

of CTEQ6.1M PDFs [17], and Q . The theoretical uncertainty of $\pm 18\%$ on $\sigma(\tilde{t}_1\bar{\tilde{t}}_1)$ is due to the choice of Q (varying the scale from its nominal value by a factor of two or a half) and PDFs. Taking this uncertainty into consideration, the limits are re-evaluated and are shown in Fig. 2 using a dashed line. The corresponding mass limits for the first and second cases are 156 GeV/ c^2 (compared to 122 GeV/ c^2 [10]) and 153 GeV/ c^2 respectively.

In conclusion, we have searched for $\tilde{t}_1\bar{\tilde{t}}_1$ production in the final state of a lepton (e or μ), a hadronically decaying tau, and two jets using 322 pb $^{-1}$ of $p\bar{p}$ collision data at $\sqrt{s} = 1.96$ TeV. We observed no excess of events in data over the number of expected events from SM processes. In an \mathcal{R}_p SUSY scenario, we set a 95% C.L. lower limit on the \tilde{t}_1 mass of 153 GeV/ c^2 taking into account the theoretical uncertainties on the NLO cross section and assuming $\mathcal{B}(\tilde{t}_1 \rightarrow \tau b) = 1$. These results are also applicable to LQ_3 pair production.

We thank the Fermilab staff and the technical staffs of the participating institutions for their vital contributions. This work was supported by the U.S. Department

of Energy and National Science Foundation; the Italian Istituto Nazionale di Fisica Nucleare; the Ministry of Education, Culture, Sports, Science and Technology of Japan; the Natural Sciences and Engineering Research Council of Canada; the National Science Council of the Republic of China; the Swiss National Science Foundation; the A.P. Sloan Foundation; the Bundesministerium für Bildung und Forschung, Germany; the Korean Science and Engineering Foundation and the Korean Research Foundation; the Science and Technology Facilities Council and the Royal Society, UK; the Institut National de Physique Nucleaire et Physique des Particules/CNRS; the Russian Foundation for Basic Research; the Comisión Interministerial de Ciencia y Tecnología, Spain; the European Community's Human Potential Programme; the Slovak R&D Agency; and the Academy of Finland.

-
- [1] H.P. Nilles, Phys. Rept. **110**, 1 (1984); H.E. Haber and G.L. Kane, *ibid.* **117**, 75 (1985).
 - [2] K. Inoue, A. Kakuto, H. Komatsu, and S. Takeshita, Prog. Theor. Phys. **68**, 927 (1982); *ibid.* **70**, 330 (1983); L.E. Ibanez and C. Lopez, Nucl. Phys. B **233**, 511 (1984); J.R. Ellis and S. Rudaz, Phys. Lett. B **128**, 248 (1983).
 - [3] A. Alves, O. Eboli, and T. Plehn, Phys. Lett. B **558**, 165 (2003).
 - [4] S. Weinberg, Phys. Rev. D **26**, 287 (1982); G.R. Farrar and S. Weinberg, *ibid.* **27**, 2732 (1983); S. Dawson, Nucl. Phys. B **261**, 297 (1985). For a recent review on RPV SUSY, see R. Barbier *et al.*, Phys. Rept. **420**, 1 (2005).
 - [5] F. de Campos *et al.*, arXiv:hep-ph/9903245; D. Restrepo, W. Porod, and J. W. F. Valle, Phys. Rev. D **64**, 055011 (2001); S. P. Das, A. Datta, and S. Poddar, Phys. Rev. D **73**, 075014 (2006).
 - [6] For a review on leptoquark models, see S. Davidson, D. C. Bailey, and B. A. Campbell, Z. Phys. C **61**, 613 (1994).
 - [7] V. M. Abazov *et al.* (D0 Collaboration), Phys. Lett. B **638**, 119 (2006). For example, the difference in $\sigma(\tilde{t}_1\tilde{t}_1)$ for the case of gluino mass of 200 GeV/ c^2 and the case of a very heavy gluino is 3% (for $m(\tilde{t}_1) = 150$ GeV/ c^2).
 - [8] D.E. Acosta *et al.* (CDF Collaboration), Phys. Rev. D **71**, 032001 (2005).
 - [9] We use a coordinate system where θ and ϕ are the polar and azimuthal angles, respectively, with respect to the proton beam direction (z axis). The pseudorapidity η is defined as $-\ln[\tan(\theta/2)]$. The transverse momentum of a particle is denoted as $p_T = p \sin \theta$. Similarly, the transverse energy is defined as $E_T = E \sin \theta$. The uncorrected missing transverse energy, \cancel{E}_T^{unc} , is the magnitude of $\vec{\cancel{E}}_T^{unc} \equiv -\sum E_T^i \hat{n}_i$, where \hat{n}_i is the unit vector in the transverse plane pointing from the interaction point to the energy deposition in calorimeter cell i . \cancel{E}_T is \cancel{E}_T^{unc} further corrected for the muon p_T and for the effects of non-ideal response of the calorimeter to e , τ , and jets.
 - [10] D.E. Acosta *et al.* (CDF Collaboration), Phys. Rev. Lett. **92**, 051803 (2004).
 - [11] A. Anastassov *et al.* (CDF Collaboration), Nucl. Instrum. Meth. A **518**, 609 (2004).
 - [12] D. Acosta *et al.*, Nucl. Instrum. Methods A **494** (2002) 57; S. Klimenko *et al.*, FERMILAB-FN-0741 (2003).
 - [13] A. Abulencia (CDF Collaboration), Phys. Rev. D **75**, 092004 (2007).
 - [14] V. Khotilovich, Ph.D. Thesis, Texas A&M University (unpublished).
 - [15] T. Sjöstrand *et al.*, Comput. Phys. Commun. **135**, 238 (2001). We use PYTHIA version 6.216.
 - [16] R. Brun *et al.*, CERN-DD-EE-81-1 (1989).
 - [17] J. Pumplin *et al.* (CTEQ Collaboration), J. High Energy Phys. **0207**, 012 (2002).
 - [18] A. Abulencia *et al.* (CDF Collaboration), J. Phys. G **34**, 2457 (2007).
 - [19] M. Cacciari *et al.*, J. High Energy Phys. **0404**, 068 (2004); N. Kidonakis and R. Vogt, Phys. Rev. D **68**, 114014 (2003).
 - [20] J.M. Campbell and R.K. Ellis, Phys. Rev. D **60**, 113006 (1999).
 - [21] F. Abe *et al.* (CDF Collaboration), Phys. Rev. Lett. **78**, 2906 (1997); G. Abbiendi *et al.* (OPAL Collaboration), Eur. Phys. J. C **31**, 281 (2003).
 - [22] W. Beenakker, R. Hopker, M. Spira, and P. M. Zerwas, Nucl. Phys. B **492**, 51 (1997).